arXiv:1601.04092v2 [astro-ph.GA] 2 Sep 2016

# On the Star Formation Properties of Void Galaxies

Crystal M. Moorman[1], Jackeline Moreno, Amanda White[2], Michael S. Vogeley

*Department of Physics, Drexel University, 3141 Chestnut Street, Philadelphia, PA 19104*

crystal.m.moorman@drexel.edu

Fiona Hoyle

*Pontifica Universidad Catolica de Ecuador, 12 de Octubre 1076 y Roca, Quito, Ecuador*

and

Riccardo Giovanelli, Martha P. Haynes

*Center for Radiophysics and Space Research, Space Sciences Building, Cornell University Ithaca, NY 14853*

## ABSTRACT

We measure the star formation properties of two large samples of galaxies from the SDSS in large-scale cosmic voids on time scales of 10 Myr and 100 Myr, using H$\alpha$ emission line strengths and GALEX *FUV* fluxes, respectively. The first sample consists of 109,818 optically selected galaxies. We find that void galaxies in this sample have higher specific star formation rates (SSFRs; star formation rates per unit stellar mass) than similar stellar mass galaxies in denser regions. The second sample is a subset of the optically selected sample containing 8070 galaxies with reliable H I detections from ALFALFA. For the full H I detected sample, SSFRs do not vary systematically with large-scale environment. However, investigating only the H I detected dwarf galaxies reveals a trend towards higher SSFRs in voids. Furthermore, we estimate the star formation rate per unit H I mass (known as the star formation efficiency; SFE) of a galaxy, as a function of environment. For the overall H I detected population, we notice no environmental dependence. Limiting the sample to dwarf galaxies still does not reveal a statistically significant difference between SFEs in voids versus walls. These results suggest that void environments, on average, provide a nurturing environment for dwarf galaxy evolution allowing for higher specific star formation rates while forming stars with similar efficiencies to those in walls.

*Subject headings:* galaxies: star formation cosmology: large-scale structure of the universe – cosmology: observations

---

[1]Physics Department, Lynchburg College, 1501 Lakeside Drive, Lynchburg, VA 24551

[2]American Museum of Natural History, Central Park West & 79th St, New York, NY 10024

## 1. INTRODUCTION

Large-scale cosmic voids make up about 60% of the volume of our Universe (Geller & Huchra 1989; da Costa et al. 1988; Pan et al. 2012). While not completely empty, these voids are underdense enough that gas-stripping galaxy interactions are exceptionally rare, making these voids a unique environment for studying the formation and evolution of galaxies. According to $\Lambda$ Cold Dark Matter ($\Lambda$CDM) simulations (e.g. Hoeft et al. (2006)), voids should have a density of low-mass halos of about 1/10th the cosmic mean. Karachentsev et al. (2004) find that the measured density of observed bright galaxies in the Local Void closely matches this prediction, but the density of dwarf galaxies in the Local Void is measured to be 1/100th that of the cosmic mean.

A posible explanation for this lack of low-mass, faint galaxies is that void dwarf galaxies may have their star formation suppressed (e.g. Koposov et al. 2009). One critical test of comparison between simulations and observations is through the relation of the predicted dark matter halo mass function and the observed galaxy luminosity and/or mass functions. Both simulations and semi-analytic models apply methods of star formation suppression to simulated dwarf "galaxies" in attempt to more closely match observations. Semi-analytic models (e.g. Benson et al. (2002)) suggest that reionization could suppress the dwarf galaxies. On the other hand, Hoeft et al. (2006) find in hydrodynamic simulations that adding in effects of UV photo-heating before and after reionization is not enough to match the slope of the observed mass function. Simulations more targeted at determining effects of large-scale environment on galaxies include the high resolution hydrodynamical simulations of void and cluster environments by Cen (2011). This adaptive mesh refinement simulation is the strongest predictor of void dwarf galaxy properties to date. The simulation predicts void dwarf galaxies at $z = 0$ will have high specific star formation rates. It predicts that these void dwarf galaxies are able to continue forming stars, because the entropy of the gas in voids is below the threshold at which the galaxies' cooling times exceeds a Hubble time.

Previous studies based on galaxy surveys suggest that galaxies within voids have higher star formation rates per stellar mass (specific star formation rate; SSFR) than galaxies in walls. Rojas et al. (2005) use a sample of $\sim$ 1000 underdense SDSS galaxies, corresponding to $\delta\rho/\rho < -0.6$, and find that void galaxies have higher SSFRs given their stellar mass. von Benda-Beckmann & Müller (2008) find stronger star formation suppression in the field than in voids using a sample of faint galaxies from the 2dFGRS. These authors also find that galaxies towards void centers have a weak tendency to have higher rates of star formation. In contrast, using a collection of 60 targeted H I imaged galaxies from the Void Galaxy Survey (VGS; Stanonik et al. 2009; Kreckel et al. 2011, 2012), Kreckel et al. (2012) find SSFRs of their void galaxies to be similar to SSFRs of galaxies from GALEX Arecibo SDSS Survey (GASS; Catinella et al. 2010) in average environments. It is important to note that H I selection has a strong effect on the sample. Ricciardelli et al. (2014) compare optically selected galaxies from within the "maximal spheres" of voids to a sample of "shell" galaxies and find no environmental dependence on SSFR. Environmental-based results from any work are certainly sensitive to the author's definition of environment. Icke (1984) and van de Weygaert & van Kampen (1993) show that voids evolve to become more spherical with time; however,

current measurements of actual voids from Pan (2011) show that voids are more ellipsoidal with a tendency to be prolate. The use of spheres and spherical shells to define environment in Ricciardelli et al. (2014) results in the "shell" sample potentially being contaminated by void galaxies. It is, therefore, unsurprising that Ricciardelli et al. (2014) find no environmental dependence on SSFR. We discuss these results in more detail in Section 7.

Overall, it seems that void galaxies tend to have higher SSFRs than galaxies in average density regions (Rojas et al. 2005; von Benda-Beckmann & Müller 2008). Thus, we wonder if there is a trend in how efficiently galaxies are converting their gas into stars across environments, allowing void dwarf galaxies to continue their star formation at late times. The efficiency with which a galaxy transforms its gas into stars is called Star Formation Efficiency (SFE) and is defined as the SFR normalized by the H I mass of the galaxy (SFE=SFR/$M_{HI}$). To determine how effectively galaxies are forming stars from their gas, we require an H I mass for each galaxy. This requirement will impose an H I selection bias on our sample, so we must carefully examine what effect H I selection has on SFRs, before making environmental comparisons.

H I surveys typically detect blue, gaseous, actively star forming galaxies. Huang et al. (2012a) find that selecting only H I detections results in overall higher SSFRs than an optically selected sample. This is due primarily to the removal of most passive (inactive) galaxies from the optically selected sample. Kreckel et al. (2012) study the efficiency of galaxies in the VGS and find two galaxies with which they can compare to similar stellar mass galaxies in denser regions. These two galaxies happen to have higher SFEs than the GASS galaxies to which they compare their observations. This hints that void galaxies *may* have higher SFEs than galaxies in average environments, but strong conclusions cannot be made with a sample of only two galaxies.

In this paper, we present the environmental effects on the specific star formation rate and the star formation efficiency of dwarf galaxies in voids using optical data from the SDSS DR8, H I data from the ALFALFA Survey, and UV data from GALEX. For the first time, we determine the large-scale environmental impact on the star formation properties of dwarf galaxies down to $M_r = -13$. Throughout this work, we assume $\Omega_m = 0.26$ and $\Omega_\Lambda = 0.74$ when calculating comoving coordinates.

## 2. NASA-Sloan Atlas

The parent data set that we use in this work is the NASA-Sloan Atlas (NSA) version (Blanton et al. 2011). The NSA is a collection of galaxies in the local Universe ($z \leq 0.055$) based primarily on the Sloan Digital Sky Survey Data Release 8 (SDSS DR8) spectroscopic catalog (York et al. 2000; Aihara et al. 2011) and contains about 140,000 galaxies within the footprint of SDSS DR8. The catalog contains galaxy parameters and images from a combination of several catalogs across multiple wavelengths: SDSS DR8, NASA Extragalactic Database, Six-degree Field Galaxy Redshift Survey, Two-degree Field Galaxy Redshift Survey, ZCAT, WISE, 2MASS, GALEX, and ALFALFA.

The NSA catalog re-analyzes the SDSS photometry in $u, g, r, i$, and $z$ bands using the background subtraction methods described in Blanton et al. (2011). The photometry is redone to help eliminate the contamination of a dwarf galaxy sample by shredded or deblended galaxies as well as to improve background subtraction procedures for large galaxies. The spectroscopic data is also re-analyzed using methods of Yan (2011) and Yan & Blanton (2012). Distances within this catalog are obtained using the local velocity flow model of Willick et al. (1997). Stellar masses in the catalog were estimated from K-correction fits (Blanton & Roweis 2007).

### 2.1. SDSS DR8

To determine SFRs on time scales of 10 Myr, we use the strength of the H$\alpha$ emission line, which we obtain from the SDSS DR8 parameters provided within the NSA. The SDSS is a wide-field multi-band imaging and spectroscopic survey that uses drift scanning to map about a quarter of the northern sky. SDSS employs the 2.5m telescope at Apache Point Observatory in New Mexico, allowing it to cover $\sim 10^4$ deg$^2$ of the northern hemisphere in the five band SDSS system–$u, g, r, i$, and $z$ (Fukugita et al. 1996; Gunn et al. 1998). Galaxies with Petrosian $r$-band magnitude $r < 17.77$ are selected for spectroscopic follow up (Lupton et al. 2001; Strauss et al. 2002). SDSS spectra are taken using two double fiber-fed spectrographs and fiber plug plates covering a portion of the sky 1.49° in radius with a minimum fiber separation of 55 arcseconds (Blanton et al. 2003). The SDSS DR8 spectra used in the NSA were reduced using the Princeton spectroscopic reduction pipeline. Flux measurements for this catalog were estimated using the code from Yan (2011) that calibrates the flux by matching the synthetic $r$-band magnitude to the apparent $r$-band fiber magnitude and subtracts the stellar continuum modeled in Bruzual & Charlot (2003). These methods are detailed in Yan (2011) and Yan & Blanton (2012).

### 2.2. GALEX

To determine SFRs on timescales of 100 Myr, we need photometric information in the far and near ultraviolet bands ($FUV$ and $NUV$, respectively). To obtain this information, we utilize data from the Galaxy Evolution Explorer (GALEX) (Martin et al. 2005). GALEX is an 0.5m orbiting space telescope that images the sky in $FUV$ and $NUV$ photometric bands across 10 billion years of cosmic history. Portions of the GALEX GR6 footprint overlap with the northern sky surveyed in SDSS DR8. In this work, we use the cross-matched NSA-GALEX GR6 catalog provided by the NSA team to obtain all UV parameters.

### 2.3. ALFALFA

To determine whether galaxies in voids are more efficient at forming stars than galaxies of similar mass in denser regions, we need an estimate of each galaxy's H I mass. We utilize the Arecibo Legacy Fast ALFA (ALFALFA) Survey (Giovanelli et al. 2005b,a) to obtain H I information for our galaxies. ALFALFA is a large-area, blind extragalactic H I survey that will detect over 30,000 sources out to $z \sim 0.06$ with a median redshift of $z \sim 0.027$, over 7000 deg$^2$ of sky upon completion. ALFALFA has a $5\sigma$ detection limit of 0.72 Jy km s$^{-1}$ for a source with a profile width of 200 km s$^{-1}$ (Giovanelli et al. 2005b) allowing for the detection of sources with H I mass down to $M_{HI} = 10^8 M_\odot$ out to 40 Mpc. At a redshift of $z \sim 0.02$, the distance out to which we can observe dwarf galaxies, ALFALFA allows for the detection of H I masses down to $M_{HI} = 10^{8.63} M_\odot$ for sources with a profile width of 200 km s$^{-1}$.

We use the most recent release of the ALFALFA Survey, $\alpha.40$ (Haynes et al. 2011), which covers $\sim$2800 deg$^2$. For this work, we are interested in sources lying in the Northern Galactic Hemisphere within $z = 0.05$. The $\alpha.40$ catalog overlaps this region in two strips in the R.A. range $07^h30^m$ <R.A.< $16^h30^m$: $04^\circ <$ Dec< $16^\circ$ and $24^\circ <$ Dec $< 28^\circ$. This region contains 8,070 H I detections within this volume. Each detection in the catalog is flagged as either Code 1, 2, or 9. Code 1 objects are reliable detections with S/N $> 6.5$; Code 2 objects have S/N< 4.5, but coincide with optical counterparts with known redshift similar to H I detection redshift; and Code 9 objects correspond to high velocity clouds. An ALFALFA team member checked the cross-matching between ALFALFA and SDSS DR7 for each H I source using information about each galaxy's color, morphology, redshift, etc. In this work, we only consider Code 1 and Code 2 detections. We use the H I masses from this catalog (which utilize the heliocentric distances provided in the catalog assuming $h = 0.7$) and use the NSA catalog for estimates of all other properties such as position, distance, and color. Because a blind H I survey is biased towards detecting blue, faint, gaseous galaxies and because the survey volume covered by ALFALFA is substantially smaller than the full NSA survey volume, only a small fraction of galaxies in the NSA catalog have H I information. Thus, we will separately track the effects of using an H I selected sample starting in Section 4.

## 3. DETERMINING ENVIRONMENT

### 3.1. Creating the Void and Wall Samples

We identify the large-scale environment of our sources by comparing the comoving coordinates of each galaxy to the void catalog of Pan et al. (2012). This void catalog uses VoidFinder, the galaxy-based void finding algorithm of Hoyle & Vogeley (2002) (also see El-Ad & Piran 1997). The algorithm grows spheres in the most underdense regions of a volume limited distribution of galaxies. Each sphere must live fully within the SDSS DR7 survey mask and must have radius $R \geq 10\mathrm{h}^{-1}$Mpc. If the volume of any two given spheres overlap by at least 10 percent, we say that

the two spheres are associated with the same void. By merging the individual spheres, we allow VoidFinder to identify non-spherical voids. When physically comparing the location of our galaxies to the identified voids, we exclude galaxies living along the edge of the survey, because we cannot determine the true large-scale structure of galaxies on the survey boundaries (see Pan et al. 2012, Hoyle et al. 2012, or Moorman et al. 2014 for a more detailed explanation). Galaxies identified as residing in a void are called void galaxies; those outside of voids are deemed wall galaxies. From the galaxies within $z < 0.05$ with H$\alpha$ line fluzes in the NSA catalog, we identify 34,548 (31%) void galaxies, 70,950 (65%) wall galaxies, and 4,320 (4%) galaxies lying on the edge of the survey mask (unclassifiable as void or wall).

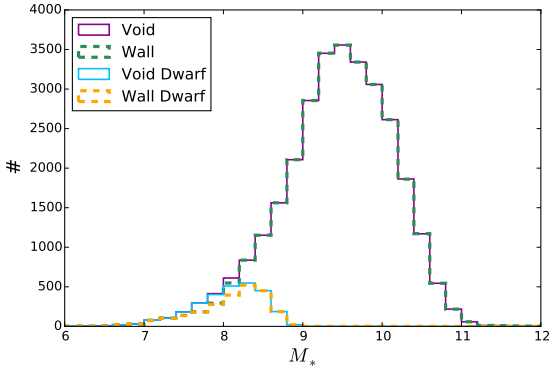


Fig. 1.— Distribution of stellar masses of the void and wall galaxies in the NSA full and dwarf samples after sparse sampling. The wall galaxies are sparse-sampled so that the stellar mass distribution matches that of the voids. Because the void stellar mass distribution is naturally shifted towards lower masses, we find fewer wall galaxies than void galaxies at the low-mass end. Thus the void and wall stellar mass distributions are not identical at the low-mass end.

Galaxies in voids are fainter and less massive than galaxies in denser regions. The characteristic luminosity of the void luminosity function shifts toward fainter luminosities by a factor of $\sim 2.5$ (Hoyle et al. 2005 and Moorman et al. 2015), and the characteristic H I mass shifts toward lower H I masses in the void H I mass function (Moorman et al. 2014). Additionally, Goldberg & Vogeley (2004) predict that the Dark Matter Halo mass functions shift toward lower masses in voids and measure this shift in Goldberg et al. (2005). This dependence of the mass/luminosity function on large-scale environment is now firmly established. Alpaslan et al. (2015) have shown that stellar mass is a strong predictor of galaxy properties. It is well established that voids host fainter, less massive galaxies. In this analysis, we would like to determine if environment has an effect on the SFE of galaxies. To test for effects of large-scale environment beyond the differences in stellar mass distributions between voids and walls, we randomly sample galaxies from the wall distribution such that the new stellar mass distribution of the wall galaxies matches that of the void galaxies. See Figure 1 for the stellar mass-matched distributions of the full NSA sample and the dwarf-galaxy-only sample. As mentioned above, void galaxies are typically less massive than wall galaxies. Therefore, in some of the lowest mass bins, we have more void galaxies than wall galaxies. When

we downsample the wall distribution, the lack of a sufficient sample of wall galaxies in these bins causes a very minor mismatch in the stellar mass distribution at masses lower than $\log(M_*) \sim 8$. Downsampling the wall galaxy sample to match the stellar mass distribution of void galaxies also removes the bias towards brighter galaxies in the walls as seen in the left panel of Figure 2. In the right panel of Figure 2, we see the effects of down-sampling the walls on $u - r$ color. Compared to the original optical color distributions seen in the walls (scaled by 0.75 and depicted as a gray dotted line in the figure), we see a decreased ratio of red to blue galaxies in walls, although not as low as that of the void sample. Similarly, stellar mass matching the wall dwarf distribution to match the void dwarf stellar mass distribution decreases the red galaxy population in the wall dwarf sample. (For wall dwarfs, we provide the original wall dwarf distribution as a scaled gray dotted line in the figure.)

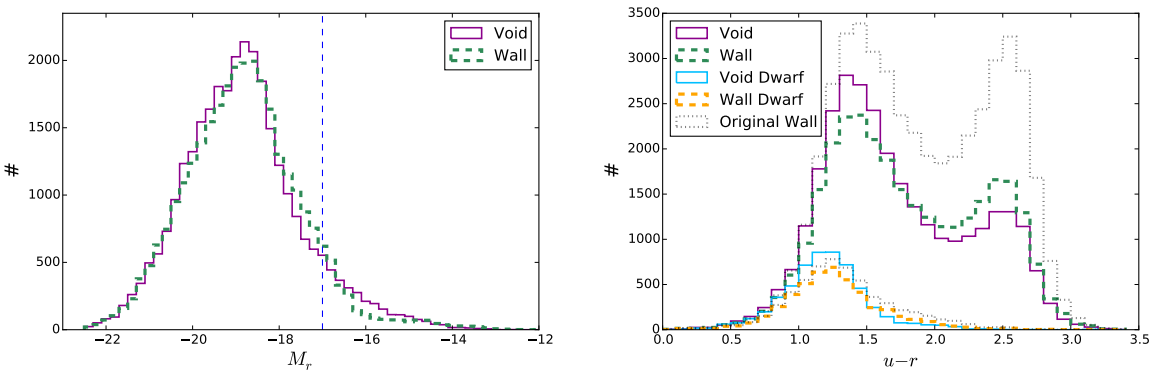


Fig. 2.— Left: Distribution of absolute magnitude $M_r$ of void and wall samples that have the same stellar mass distribution. The bias towards brighter galaxies in walls is largely removed. The blue dashed line indicates the division between dwarf galaxies and brighter galaxies. Right: Distribution of $u - r$ color of void and wall samples that have the same stellar mass distribution. The number of red galaxies within the walls is reduced, but there is still a higher ratio of red to blue galaxies in walls than voids. For clarity, the dwarf distributions have been amplified by a factor of 2.

Of the galaxies with H I information, we find 2,737 (34%) void galaxies and 5,154 (64%) wall galaxies within $z < 0.05$. The remaining (2%) lie along the survey edges and are excluded due to the potential misclassification issues. We apply the same stellar mass-matched requirements to the H I sample as discussed earlier. The stellar mass matching has similar effects on the H I sample distributions. The $M_r$ distributions of void and wall samples become more similar. The $u - r$ distribution of the wall galaxies becomes less red overall. By its nature, the H I sample primarily selects primarily blue, gas-rich galaxies (Toribio et al. 2011; Huang et al. 2012a; Moorman et al. 2015). Because H I selection preferentially selects gas-rich galaxies, we expect the wall galaxies in this sample to be primarily late-type galaxies, more similar to void galaxies than the full population of optically selected, wall galaxies. Additionally, the stellar mass matching accounts for the well-known shift towards less massive galaxies in voids; therefore, we do not expect that we will see much of a difference between the star formation properties of the H I selected void and H I selected

wall galaxies.

### 3.2. Creating the Small-Scale Density Samples

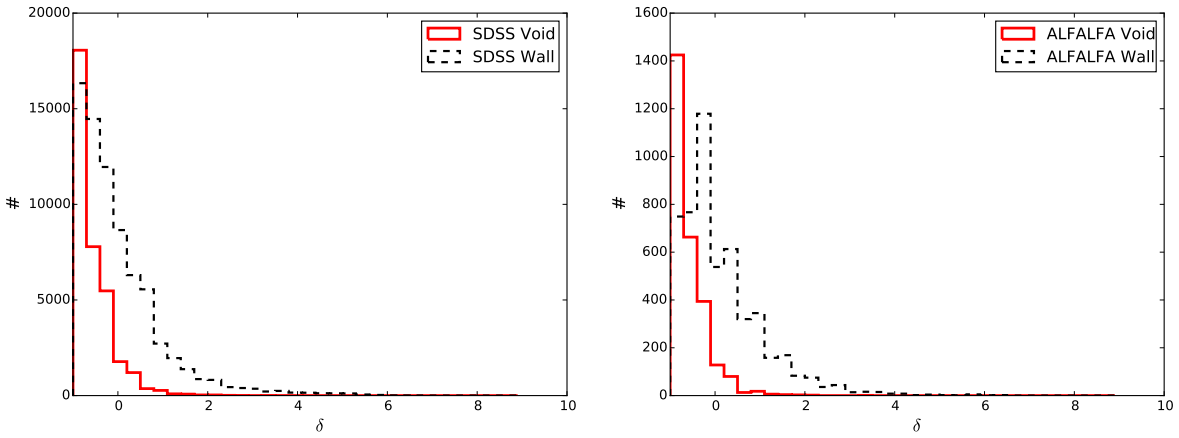


Fig. 3.— Distribution of relative local densities for void and wall galaxies in the NSA (left) and ALFALFA (right) samples. Void and wall galaxies were selected using a volume-limited sample based on $M_r = -20.1$, whereas the small scale densities were calculated using a volume-limited sample based on $M_r = -18.5$. We see that wall galaxies range anywhere from isolated to clustered regions. Our void galaxies are grouped together with relatively fainter galaxies ($-20.1 < M_r < -18.5$) within the voids on smaller scales than are probed by the void catalog.

Previous work indicates that star formation properties may be influenced by local density. For example, Elbaz et al. (2007) find that galaxy SSFRs decrease with stellar mass and increase with density at $z \sim 1$. Huang et al. (2012b) find that low H I mass ALFALFA detections ($M_{HI} < 10^{7.7}$) in the Virgo Cluster have gas depletion time scales less than a Hubble time. This implies that either the dwarf galaxies are undergoing gas-stripping interactions (common to galaxy clusters) or the highest density regions are somehow enhancing SFEs.

In Section 6, we study the effects of local density on SFE in ALFALFA galaxies. We estimate the small-scale densities of each galaxy within the volume covered by VoidFinder, based on a volume-limited sample from the SDSS DR7 KIAS-VAGC (Choi et al. 2010) catalog. We create a volume-limited sample with an absolute magnitude cut of $M_r = -18.5$ corresponding to a redshift cut of $z = 0.06$ to ensure that we completely enclose the NSA volume ($z_{max} = 0.055$). We apply a nearest-neighbors algorithm to the volume-limited sample with a smoothing scale of $\sim 2.5$ $h^{-1}$Mpc to approximate the local density, $\rho$, within the volume covered. We then evaluate the relative local density of each galaxy in the NSA catalog mentioned above. Figure 3 shows the distribution of our void and wall galaxies as a function of small-scale density contrast, $\delta = (\rho - \bar{\rho})/\bar{\rho}$. We find that void galaxies typically lie in regions where the local density contrast is less than the mean,

but there may be filaments or groups of $M_r \leq -18.5$ galaxies within the voids increasing the local densities within the voids. Additionally, we find wall galaxies with small $\delta$ that are not located in large-scale voids.

## 4. ESTIMATING STAR FORMATION PROPERTIES

To determine if large-scale environment affects star formation in galaxies, and on what time scales, we measure the star formation rate (SFR) of galaxies using two independent methods. The first method, described in detail in Salim et al. (2007), uses $FUV$ photometry. $FUV$ photometry depends primarily on O- and B-type stars with masses $M \gtrsim 3M_\odot$ and lifetimes less than $\sim 300$ Myr. Therefore, the $FUV$ method best estimates the star formation rates of galaxies over the past $\sim 100$ Myr. The second method is described in Lee et al. (2009) and measures SFRs using H$\alpha$ spectral lines. Only massive ($> 10\ M_\odot$), young ($< 20$ Myr) stars (O-type stars) significantly contribute to the integrated ionizing flux of a galaxy; thus, the H$\alpha$ method provides a good estimate of SFRs on short timescales ($\sim 10$ Myr). Both of these methods use the star formation relations of Kennicutt (1998). We briefly describe the methods in this section.

### 4.1. $FUV$ Method

We measure the SFRs of galaxies over the last 100 Myr using the GALEX photometric $FUV$ fluxes from the NSA catalog. $FUV$ photometry is sensitive to dust; therefore, we correct the rest frame $FUV$ fluxes for dust attenuation. We do so via the empirical equations found from SED fitting of GALEX galaxies in Salim et al. (2007). These authors find the effects of dust are stronger for red ($NUV - r \geq 4$) galaxies than blue ($NUV - r < 4$) galaxies. Thus red galaxies are corrected by

$$A_{FUV} = \begin{cases} 3.32(FUV - NUV) + 0.22 & FUV - NUV \leq 0.95 \\ 3.37 & FUV - NUV > 0.95 \end{cases}, \tag{1}$$

and blue galaxies are corrected by

$$A_{FUV} = \begin{cases} 2.99(FUV - NUV) + 0.27 & F - N \leq 0.90 \\ 2.96 & F - N > 0.90 \end{cases}. \tag{2}$$

Here, $A_{FUV}$ is the dust attenuation correction for SFRs obtained using the $FUV$ method. For galaxies with dust attenuation corrections falling below zero, we set the correction to $A_{FUV} = 0$, to ensure that we are not artificially adding dust back into the system. We apply this correction to the rest-frame flux, $f^0$, in the following way:

$$f_{FUV} = f^0 10^{A_{FUV}/2.5}. \tag{3}$$

From the dust corrected $FUV$ fluxes, $f_{FUV}$, we calculate the $FUV$ luminosities via

$$L_{FUV} = 4\pi D_L^2 f_{FUV}, \tag{4}$$

where $D_L$ is the luminosity distance. Following Salim et al. (2007), we then apply the Kennicutt (1998) SFR relation with a factor to better match the stellar evolution models of Bruzual & Charlot (2003),

$$SFR = 1.08 \times 10^{-28} L_{FUV}, \tag{5}$$

to obtain the average SFR in units of $M_\odot \mathrm{yr}^{-1}$ over the past $\sim 100$ Myr.

### 4.2. H$\alpha$ Method

For an estimate of galaxy SFRs over the last $\sim 10$ Myr, we calculate the H$\alpha$ luminosity and apply the Kennicutt (1998) SFR relation similar to equation (5):

$$SFR = 7.9 \times 10^{-41.28} L_{\mathrm{H}\alpha} \tag{6}$$

to obtain the average SFR in units of $M_\odot \mathrm{yr}^{-1}$ over the past $\sim$ 10 Myr. Here, $L_{\mathrm{H}\alpha}$ is the H$\alpha$ luminosity obtained from

$$L_{\mathrm{H}\alpha} = 4\pi D_L^2 f_{\mathrm{H}\alpha}, \tag{7}$$

where $f_{\mathrm{H}\alpha}$ is the dust-corrected H$\alpha$ flux and $D_L$ is the luminosity distance. As with the $FUV$ method above, we must make dust attenuation corrections to the H$\alpha$ SFR estimates. To do so, we use the correction suggested in Lee et al. (2009):

$$A_{\mathrm{H}\alpha} = 5.91 \log(\mathrm{H}\alpha/\mathrm{H}\beta) - 2.70. \tag{8}$$

Additionally, we make an aperture correction to the H$\alpha$ luminosity to adjust for the 3" diameter SDSS fiber potentially being smaller than the size of the galaxy observed. The SDSS fiber detects H$\alpha$ emission from a fraction of the galaxy that depends on the redshift and intrinsic size of the galaxy. We use the correction of Hopkins et al. (2003) adjusting the H$\alpha$ luminosity by a factor of $10^{-0.4(r_{\mathrm{Petro}} - r_{\mathrm{fiber}})}$. Here, $r_{Petro}$ is the $r$-band Petrosian magnitude of the full galaxy, and $r_{\mathrm{fiber}}$ is the $r$-band magnitude within the fiber. This aperture correction assumes that star formation is uniformly distributed across the galaxy. Depending on galaxy orientation and non-uniform distribution of star formation activity, Hopkins et al. (2003) find that this aperture correction may over estimate the SFR by up to 15% for galaxies out to $z \sim 0.2$.

### 4.3. Star Formation Rates

We calculate the SFR for both methods mentioned above for all galaxies in our data set. The NSA catalog includes estimates of H$\alpha$ line flux and $NUV/FUV$ photometry for all galaxies. Thus,

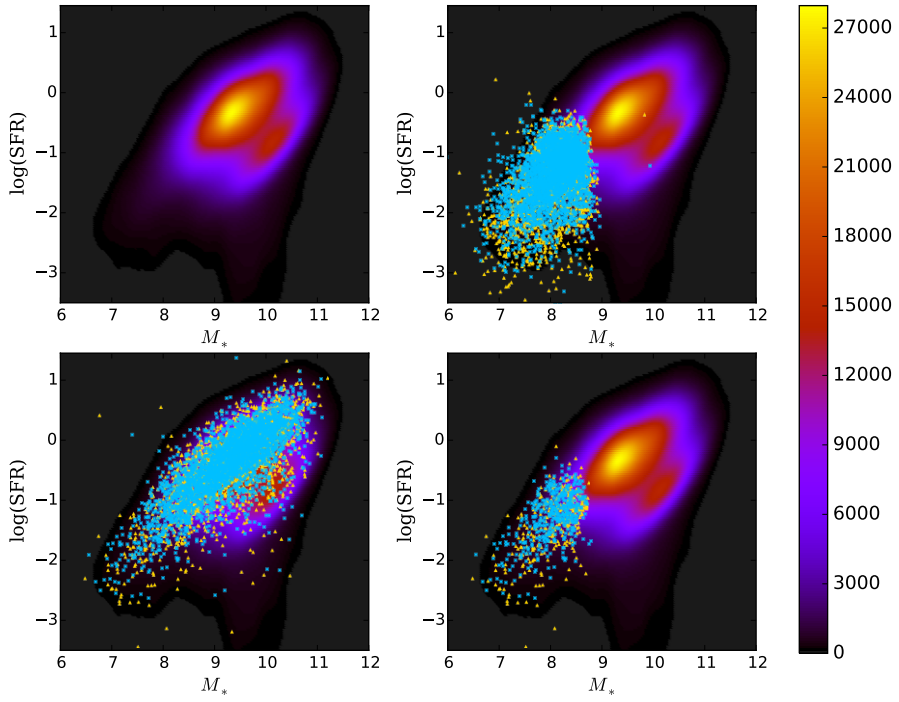


Fig. 4.— Upper Left: Color contours depict the stellar mass, $\log(M_*)$, vs $\log(\mathrm{SFR}_{FUV})$ distribution for all NSA galaxies. The colorbar indicates the number of galaxies in the sample in this space. Upper Right: NSA Dwarf void (blue crosses) and stellar mass-matched wall (gold triangles) galaxies overplotted on the full NSA distribution. SFR is closely correlated with mass; therefore, it is unsurprising that dwarf galaxies tend to have low SFRs. Most dwarf galaxies in the NSA are star forming with a small fraction appearing in an extension of the passive sequence. Lower Left: All ALFALFA void and stellar mass-matched wall galaxies. ALFALFA typically detects active star forming galaxies, mostly avoiding the passive galaxy region in the plot. Lower Right: ALFALFA Dwarf void and stellar mass-matched wall galaxies. These galaxies lie almost exclusively in the star forming sequence.

we did not exclude low SFR galaxies and there is no bias in the sample toward high SFR galaxies. In this work, we investigate the differences of the star formation properties based on environment and sample selection of the following samples: all galaxies identifiable as a void or wall galaxy (hereafter, NSA), all dwarf galaxies identifiable as a void or wall galaxy (NSA Dwarf), galaxies within the aforementioned NSA sample with ALFALFA H I masses measured with S/N>4.5 (ALFALFA), and galaxies within the NSA Dwarf sample with corresponding H I clouds with S/N>4.5 (ALFALFA Dwarf).

We investigate the effects of sample selection on SFR by comparing the location of galaxy subsamples within $\log(\mathrm{SFR}_{FUV})$ vs. stellar mass ($\log M_*$) space to the full galaxy catalog in Figure 4. Again, the NSA sample is a superset of all other galaxy samples used in this work (i.e. the NSA Dwarf, ALFALFA, and ALFALFA Dwarf samples). The upper left panel of Figure 4 depicts a density contour of the NSA sample in a $\log(\mathrm{SFR}_{FUV})$ vs. $\log(M_*)$ diagram. We see a clear bimodality in the diagram, indicating the existence of both an "active" (higher SFR) population depicted by the main peak in the contour diagram, and a "20pt" (lower SFR) population depicted by the smaller peak to the lower right of the main peak. In the lower left panel, we select galaxies within the NSA catalog with H I emission lines strong enough to be detected by ALFALFA. We divide the ALFALFA detections into void (blue crosses) and wall (yellow triangles) galaxies and overplot them on the NSA density contour in the log(SFR) vs. $\log(M_*)$ space. This panel shows the overall effects of H I selection on galaxy SFR. We notice that we lose most evidence of bimodality in the distribution. This confirms that H I surveys tend to detect galaxies that are actively forming stars today. These findings corroborate the work of Huang et al. (2012a), who mention that the ALFALFA galaxies have higher SFRs than optically selected samples from the SDSS. We see some evidence at the high stellar mass end that a population of quiescent galaxies exists that contain just enough gas to be detected by ALFALFA. Using the H$\alpha$ method rather than the $FUV$ method, we find very similar results on the sample selection effects and dwarf selection effects; thus, we will not plot the H$\alpha$ estimated SFR distributions here.

## 5. SPECIFIC STAR FORMATION RATES

SFR is correlated with stellar mass; therefore it is no surprise that selecting only the dwarf galaxies (right column of Figure 4) produces lower SFRs than the average galaxies in the full catalogs. To account for the correlation between the SFR and mass of a galaxy, we normalize the SFR of each object by its stellar mass to obtain its specific SFR ($\mathrm{SSFR}=\mathrm{SFR}/M_*$), which is a measure of the SFR per unit mass. Figure 5 depicts the location of each galaxy sample within the $\mathrm{SSFR}_{FUV}$ vs. stellar mass plane. The upper left panel shows the density contour of the NSA sample. The passive galaxy sequence is seen primarily as an extension from the main active sequence moving towards lower SSFRs around $\log(M_*) \sim 10$ and continuing towards the bottom edge of the figure. This density contour is replotted in the background of each subplot of the figure for the sake of comparing how sample selection affects the SSFRs. In the lower left panel, we

divide the ALFALFA detections into void (blue crosses) and wall (yellow triangles) galaxies and scatter them over the NSA density contour in the SSFR vs. stellar mass space. This panel shows the overall effects of H I selection on galaxy SSFR. As seen in Section 4.3, we find the ALFALFA sample lies primarily in the star forming sequence and is sparse in the passive galaxy region. Huang et al. (2012a) find a similar result for all ALFALFA galaxies.

In the right column of Figure 5, we select out only the dwarf galaxies ($M_r \geq -17$) within the NSA (top right) catalog and overplot them on the full NSA density contours. We find that, as a whole, dwarf galaxies tend to lie primarily in the active star forming sequence, with a few trailing into the passive region. Dwarf galaxies have higher SSFRs than average galaxies as predicted by the high resolution hydrodynamic simulations of Cen (2011). We then select out the dwarf galaxies that have an H I flux large enough to be detected in ALFALFA. We plot these galaxies in the bottom right panel of Figure 5, and find that the H I selection cuts out almost all of the dwarf galaxies lying in the passive galaxy region.

To quantitatively determine the large-scale environmental effects on the SSFR, we fit the *FUV* and H$\alpha$ SSFRs for the NSA and ALFALFA samples by two summed Gaussians:

$$f(x) = \frac{A_1}{\sigma_1\sqrt{2\pi}} e^{-\frac{(x-\mu_1)^2}{2\sigma_1^2}} + \frac{A_2}{\sigma_2\sqrt{2\pi}} e^{-\frac{(x-\mu_2)^2}{2\sigma_2^2}}. \quad (9)$$

Here, $A$ is the amplitude, $\mu$ is the mean, and $\sigma$ is the standard deviation of each 1-D gaussian. The two Gaussians used to fit the SSFR distributions correspond to the passive and active star forming populations of each sample. Figure 6 depicts the SSFR distributions with best-fitting summed Gaussians. See Table 1 for the best fitting Gaussian parameters for each sample.

The left panels in Figure 6 plot SSFR distributions averaged over the last $\sim 10$ Myr, estimated using the H$\alpha$ line. The right panels plot the SSFR distributions averaged over the last $\sim 100$ Myr, estimated using the *FUV* photometry. The top row shows the stellar mass-matched NSA data, and the bottom row shows the stellar mass-matched ALFALFA data. It is obvious from the top left panel of Figure 6 that void galaxies have higher SSFRs than wall galaxies in both the active (13% shift) and passive (41% shift) regions based on the H$\alpha$ estimates. For the NSA Dwarf sample, the void galaxy distribution has an 11% shift towards higher SSFRs than stellar mass-matched wall dwarf galaxies when using the H$\alpha$ method.

In the upper right panel of Figure 6, we measure the *FUV* SSFR for NSA galaxies and find that void galaxies have higher SSFRs than stellar mass-matched wall galaxies in both the active (13%) and passive (41%) populations. The NSA Dwarf void galaxies also experience higher SSFRs based on the *FUV* method by $\sim 7$%. Based on the *FUV* method, we find that 90% of void dwarf galaxies and 85% of wall dwarf galaxies have SSFRs high enough to double their stellar mass in a Hubble time (corresponding to log(SSFR)$> -10.1\ M_\odot \mathrm{yr}^{-1}$). Computing the Kolmogorov-Smirnov (K-S) test statistic on the mass-matched void and wall SSFR distributions on both time scales returns a $p$-value less than 0.001 for the NSA void and stellar mass-matched wall samples as well as for the NSA Dwarf void and stellar mass-matched wall samples. Thus, we can reject the null

Table 1. Gaussian fits to the SSFRs

| Sample | type | method | $A_1$ | $\mu_1$ | $\sigma_1$ | $A_2$ | $\mu_2$ | $\sigma_2$ |
|---|---|---|---|---|---|---|---|---|
| NSA | void | H$\alpha$ | 3841 | -9.906 | 0.651 | 926 | -11.707 | 0.518 |
| NSA | wall | H$\alpha$ | 3576 | -9.961 | 0.658 | 1194 | -11.858 | 0.489 |
| NSA Dwarf | void | H$\alpha$ | 355 | -9.752 | 0.773 | 33 | -12.029 | 0.078 |
| NSA Dwarf | wall | H$\alpha$ | 282 | -9.803 | 0.793 | 21 | -12.401 | 0.261 |
| NSA | void | *FUV* | 5406 | -9.719 | 0.454 | 1727 | -10.963 | 0.294 |
| NSA | wall | *FUV* | 4691 | -9.769 | 0.489 | 2269 | -10.970 | 0.272 |
| NSA Dwarf | void | *FUV* | 612 | -9.434 | 0.438 | — | — | — |
| NSA Dwarf | wall | *FUV* | 471 | -9.467 | 0.488 | — | — | — |
| ALFALFA | void | H$\alpha$ | 263 | -10.177 | 0.540 | 129 | -10.110 | 0.991 |
| ALFALFA | wall | H$\alpha$ | 167 | -10.199 | 0.896 | 260 | -10.104 | 0.429 |
| ALFALFA Dwarf | void | H$\alpha$ | 59 | -9.984 | 0.618 | 22 | -8.781 | 0.215 |
| ALFALFA Dwarf | wall | H$\alpha$ | 51 | -9.968 | 0.579 | 11 | -8.423 | 0.163 |
| ALFALFA | void | *FUV* | 416 | -9.633 | 0.323 | 233 | -9.697 | 0.561 |
| ALFALFA | wall | *FUV* | 449 | -9.616 | 0.331 | 181 | -9.814 | 0.618 |
| ALFALFA Dwarf | void | *FUV* | 104 | -9.378 | 0.376 | 5 | -9.114 | 0.570 |
| ALFALFA Dwarf | wall | *FUV* | 81 | -9.456 | 0.383 | 1 | -8.218 | 3.131 |

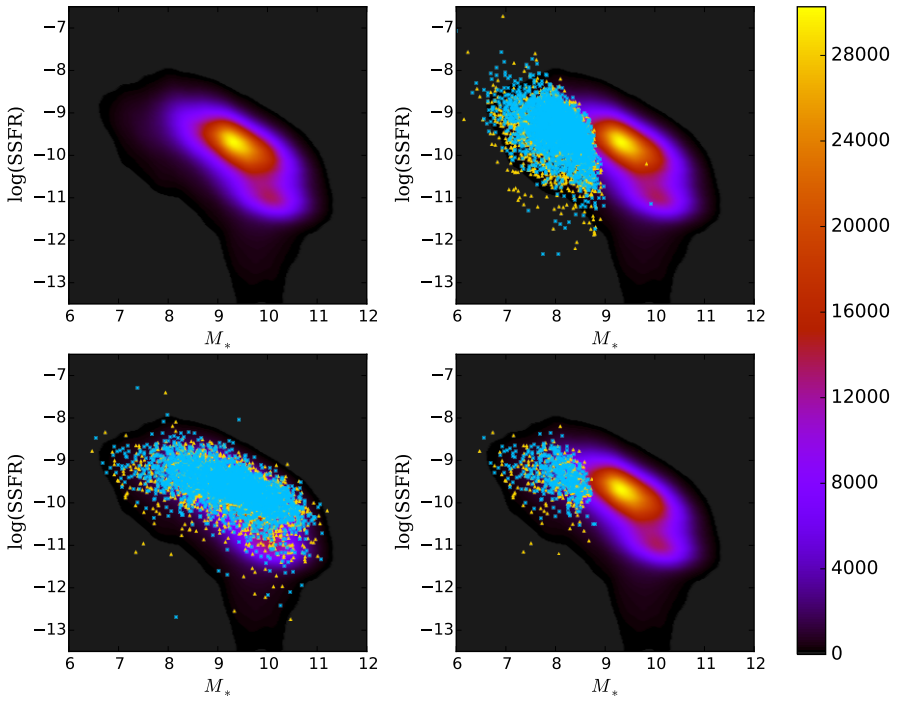


Fig. 5.— Upper Left: Color contours depict the stellar mass, $\log(M_*)$, vs $\log(\mathrm{SSFR}_{FUV})$ distribution for all NSA galaxies. The colorbar indicates the number of galaxies in the sample in this space. Upper Right: NSA Dwarf void (blue crosses) and wall (gold triangles) galaxies overplotted on the full NSA distribution. The wall dwarf galaxies have been downsampled so that the wall dwarf galaxy stellar mass distribution matches the stellar mass distribution of void dwarf galaxies. Dwarf galaxies tend to have relatively high SFRs given their size. A majority of dwarf galaxies lie in the active star forming region in this space. Lower Left: All ALFALFA void and stellar mass-matched wall galaxies. As seen with the SFR distributions, ALFALFA typically detects active star forming galaxies, avoiding the passive galaxy region in the plot. Lower Right: ALFALFA void dwarf and stellar mass-matched wall dwarf galaxies. These galaxies are actively forming stars at relatively high rates.

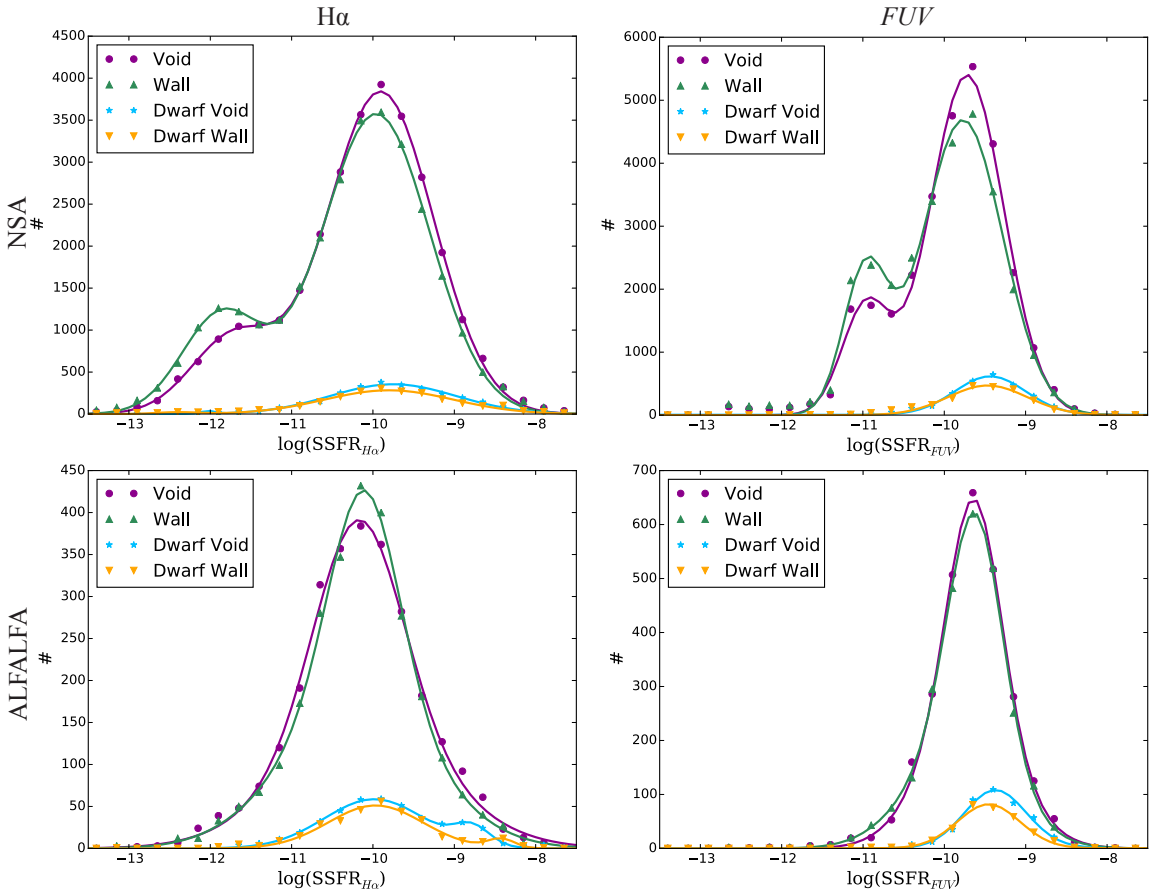


Fig. 6.— SSFR distribution of void and stellar mass-matched wall galaxies measured via H$\alpha$ and *FUV* methods for NSA, NSA Dwarf, ALFALFA, and ALFALFA Dwarf samples. Lines denote the best-fit summed Gaussian. Upper Left: NSA SSFR distributions via the H$\alpha$ method. Void galaxies have higher SSFRs than wall galaxies in the full sample as well as the dwarf sample. Upper Right: NSA SSFR distributions via the *FUV* method. Again, the void galaxies have higher SSFRs than wall galaxies in the full sample as well as the dwarf sample. Lower Left: ALFALFA SSFR distributions via the H$\alpha$ method. Due to H I selection effects, we do not see evidence of the passive galaxy sequence. We notice no difference in the full void and wall distributions. A peak in the high-SSFR end of the void dwarf distribution reveals a population of star-bursting void dwarf galaxies. Lower Right: ALFALFA SSFR distributions via the *FUV* method. There is no significant difference between the full void and wall samples. The void dwarf distribution appears to be shifted towards higher SSFRs.

hypothesis that the void and stellar mass-matched wall galaxies from these two sets were drawn from the same distribution.

### 5.1. Tracking the Sample Selection Effects

SSFRs are highly anti-correlated with $NUV-r$ color (with correlation coefficients of $r_s$=-0.923 for the NSA sample and $r_s$=-0.875 for the ALFALFA sample). That is, bluer galaxies tend to have higher SSFRs. Of course, there are always exceptions, such as the population of dust-reddened spiral galaxies detected by ALFALFA (e.g. Moorman et al. (2015)). Edge-on, blue spiral galaxies will have high SSFRs, but will generally appear redder than they truly are due to dust in the galaxy absorbing and scattering photons with shorter wavelengths. Because of the bias towards blue galaxies in the H I samples, we will see hardly any difference between the SSFRs of void and wall galaxies. On average, the SSFRs of an H I selected sample should be higher than for an optically selected sample because we are lacking galaxies from the red, passive galaxy sequence. While the average SSFRs are higher, comparing only the active star-forming sequence of ALFALFA to that of NSA reveals a shift towards lower SSFRs in H I surveys. This is unsurprising given that the ALFALFA blue cloud is shifted towards redder colors than the SDSS blue cloud (see, for instance, fig. 1 in Moorman et al. (2015)). The shift is possibly indicative of H I selected galaxies being more dust-reddened on average than optically selected star forming galaxies.

In the bottom panels of Figure 6, there are no discernible differences between the full ALFALFA void and ALFALFA stellar mass-matched wall SSFR distributions on either time scale. Estimating a shift in the void and wall distributions based on the summed Gaussian fits, we find only a 5% shift towards lower H$\alpha$ SSFRs with a broader distribution in voids than walls (see Table 1 for fits). In the bottom right panel, we find a $< 1\%$ shift towards higher $FUV$ SSFRs and no width differences in the distributions, implying that the SSFRs of H I selected galaxies are not dependent on large scale structure based on the $FUV$ method. The K-S test results in $p_{K-S} = 0.09$ for H$\alpha$ SSFRs and $p_{K-S} = 0.14$ for $FUV$ SSFRs, meaning that we cannot reject that the ALFALFA void and wall samples were drawn from the same distribution on either time scale.

Limiting our scope to the ALFALFA Dwarf sample, we find in the H$\alpha$ SSFR distribution that the main peak of the void sample, centered on log(SSFR)$\sim -10$, is shifted only by $\sim 4\%$ towards lower SSFRs than the main peak of the wall galaxy distribution. Both the void and wall ALFALFA Dwarf samples have secondary peaks at the high end of the H$\alpha$ SSFR distribution not apparent in any other sample. This is indicative of a population of star bursting dwarf galaxies that has been active very recently (10 Myr) especially in voids. The wall galaxies, however, seem to be lacking a sample of high H$\alpha$ SSFRs around $-9.2 <$log(SSFR)$< -8.4$ where the secondary void peak is strongest. This effect is most likely due to ALFALFA's bias towards detecting galaxies preferentially found in voids. At higher SSFRs, the wall dwarf distribution increases again, to closely match the void distribution around log(SSFR) $\sim -8.5$. Due to these high-SSFR features, a K-S test yields $p_{K-S} = 0.005$, indicating that we should reject that these samples are drawn from

the same population.

On longer star formation time scales ($\sim$ 100 Myr), the ALFALFA Dwarf void galaxies are shifted towards higher *FUV* SSFRs by 23% with $p_{K-S} = 0.002$. Based on this test statistic, we should reject that the void and wall ALFALFA Dwarf detections were drawn from the same distribution. Based on these SSFR results, we expect that we will find the star formation efficiency of ALFALFA void and wall galaxies to be very similar for both the H$\alpha$ and *FUV* methods. We also suspect the ALFALFA Dwarf galaxies will vary only slightly on both short and long time scales. Compared to the NSA Dwarf SSFR$_{FUV}$ distribution, the ALFALFA Dwarf galaxies have higher SSFRs on average with 94% of void dwarfs and 93% of wall dwarfs having SSFRs high enough to double their stellar mass within a Hubble time (Cen 2011).

## 6. STAR FORMATION EFFICIENCY

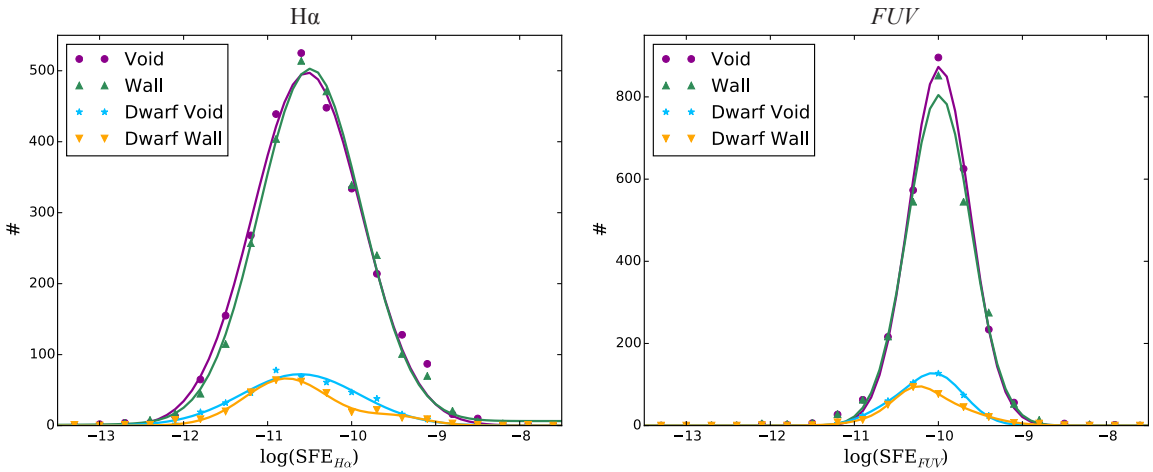


Fig. 7.— Left: Distribution of the H$\alpha$ SFE of all void and wall galaxies as well as the dwarf void and wall galaxies. Right: Distribution of the *FUV* SFE of all void and wall galaxies as well as the dwarf void and wall galaxies. There is no discernible difference between the full void and wall SFE distributions of ALFALFA galaxies on either timescale. Isolating the ALFALFA dwarf galaxies reveals a slight trend towards higher SFEs in void galaxies.

A measure of how efficiently galaxies are transforming their gas into stars is the SFR normalized by the H I mass, termed the galaxy's star formation efficiency (SFE = SFR/$M_{HI}$). In Figure 7 we present the SFE distribution of the full ALFALFA void and wall samples and the ALFALFA Dwarf void and wall samples for both the H$\alpha$ method (left panel) and *FUV* (right panel). The lines plotted represent the best-fit summed Gaussians (see Equation 9) with parameters shown in Table 2. In the H$\alpha$ distribution, we find a small (9%) shift towards lower SFEs and a broader distribution in ALFALFA void galaxies compared to walls. As with the ALFALFA Dwarf SSFR$_{\rm H\alpha}$

distributions, the $\mathrm{SFE}_{\mathrm{H}\alpha}$ wall distribution is lacking at the high SFE end ($\log(\mathrm{SFE}) \sim -10$). This is primarily due to the same large-scale structure (LSS) and H I selection effects discussed in the previous section. We also find similar results between the $\mathrm{SFE}_{FUV}$ and $\mathrm{SSFR}_{FUV}$, in that there is no difference in the ALFALFA void and wall distributions and there is a lack of ALFALFA Dwarf wall galaxies at high SSFRs. This lack of wall galaxies may be due to the prominence of nearby voids within the ALFALFA $\alpha.40$ volume. The K-S test statistics ($p_{full} = 0.13$ and $p_{dwarf} = 0.17$ for the H$\alpha$ method and $p_{full} = 0.24$ and $p_{dwarf} = 0.11$ for the $FUV$ method) indicate that we cannot reject that the samples were drawn from the same distribution.

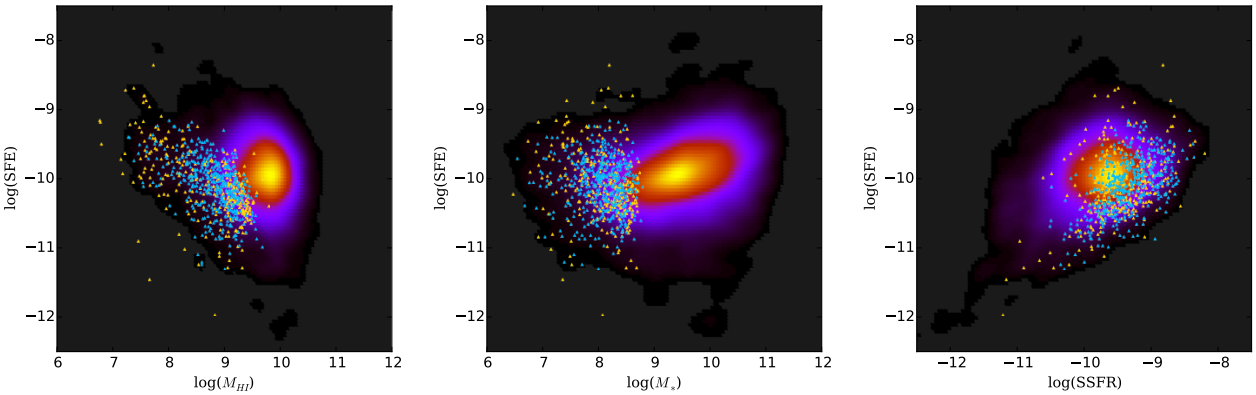


Fig. 8.— Left to right: ALFALFA galaxy SFEs as a function of $M_{HI}$, $M_*$, and SSFR. Color contours represent the full ALFALFA sample, while the ALFALFA void dwarf (blue crosses) and ALFALFA wall dwarf (gold triangles) populations are overplotted. The wall dwarf galaxies were sampled so that the wall dwarf stellar mass distribution matched the void dwarf stellar mass distribution. We notice a population of wall dwarf galaxies with very high SFEs.

Figure 8 presents the distribution of SFEs as a function of $M_{HI}$, $M_*$, and SSFR. ALFALFA Dwarf void galaxies (blue crosses) and wall galaxies (gold triangles) are overplotted on the colored-contour of the full ALFALFA sample in each space. We see evidence of a population of $\sim$ 10 low-H I mass dwarf galaxies with relatively high SFEs in walls. These 10 galaxies do not differ drastically from the other dwarf galaxies in stellar mass or SSFR. Figure 9 shows the $M_*$ vs $M_{HI}$ distribution of the ALFALFA dwarf galaxies. Huang et al. (2012a) and Kreckel et al. (2012) show that ALFALFA galaxies are predominately H I mass dominated below $\log(M_*) \sim 9.5$ (falling below the dashed line in the figure) and stellar mass dominated at larger $M_*$. The high SFE wall galaxies fall below the $M_{HI} = M_*$ line, indicating that they have lower gas mass fractions than typical ALFALFA galaxies of similar stellar mass. We note that the void and wall dwarf galaxies plotted in Figure 9 are stellar mass-matched, so the shift towards lower $M_{HI}$ at a given $M_*$ is important. Galaxies with low gas fractions typically show the following traits: low SFRs, low SSFRs, high SFEs, high metallicities, high extinctions, redder, and more evolved. These particular galaxies do have lower a SFR and SSFR, and a higher SFE, but they appear to be just as blue as the rest of the ALFALFA dwarf population and half of them are late-type while the other half are early-type

as judged by the galaxies inverse concentration index. These galaxies live in relatively high local density regions as determined by the KDE estimator discussed in Section 3 (see Figure 10 for SFEs as a function of local density).

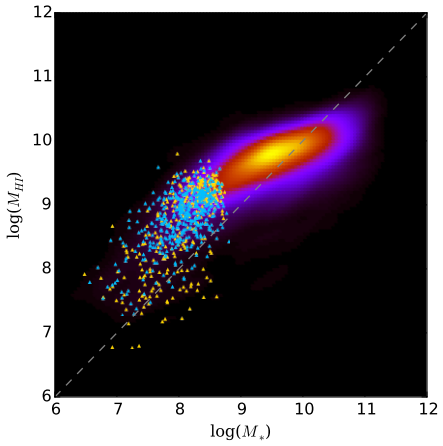


Fig. 9.— Color contours show $M_*$ vs $M_{HI}$ of the full ALFALFA sample. ALFALFA void dwarf (blue crosses) and stellar mass-matched wall dwarf (gold triangles) galaxies are overplotted. We see that at a given stellar mass, void dwarf galaxies have higher H I masses than wall dwarf galaxies. This implies that void dwarf galaxies have lower SFEs than similar stellar mass galaxies in walls.

Measured on both time scales, the SFE distribution of void dwarf galaxies appears broader than that of wall dwarf galaxies. The broadened distribution towards lower SFEs could be indicative of *marginally* lower SFEs in void dwarf galaxies. Furthermore, we see that the SFE distributions for void and wall galaxies both shift towards lower SFEs on shorter timescales, but we find no evidence of a stronger shift in either the void or wall samples. Perhaps this means the void environment does provide a sheltered life for dwarf galaxies, allowing them to retain their H I gas allowing for fueling over longer periods.

## 7. COMPARISON TO PREVIOUS RESULTS

Our results are consistent with previous studies regarding the variation of galaxy SSFRs with large-scale environment that indicate that galaxies in underdense environments have higher SSFRs than those in denser regions. Rojas et al. (2005) measure the SSFR of galaxies from an earlier data release of the SDSS and find that at fixed luminosity, void galaxies have higher SSFRs than wall galaxies. They also find that SFRs are very similar or slightly lower for void galaxies than wall galaxies, but this is expected, because void galaxies are generally less massive and SFRs are correlated with galaxy mass. Similarly, using a sample of faint galaxies from the 2dFGRS, von Benda-Beckmann & Müller (2008) find stronger star formation suppression in the field than in voids via the color-SSFR relation. That is, they find that galaxy colors are redder in denser regions

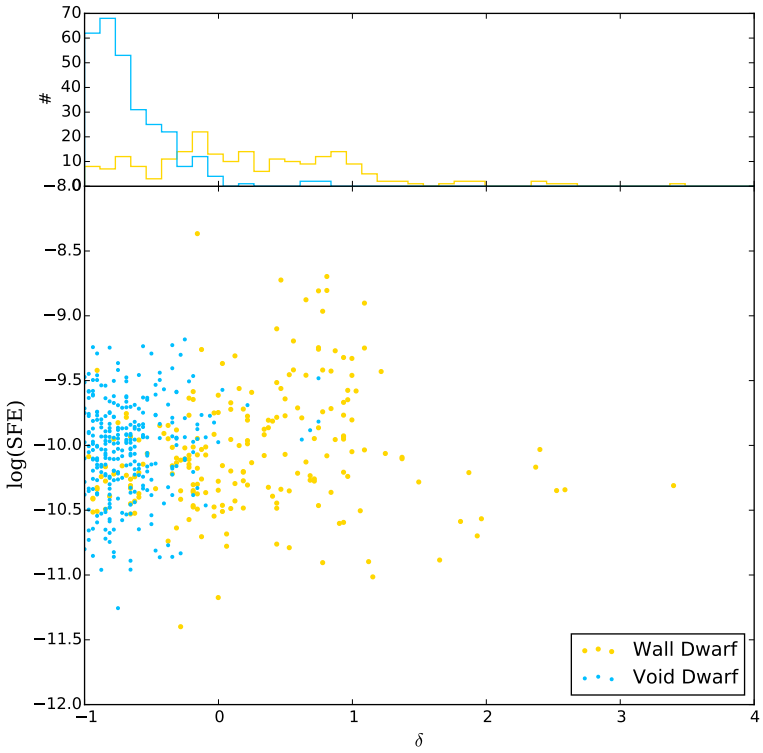


Fig. 10.— SFEs for void dwarf (blue) and stellar mass-matched wall dwarf (gold) galaxies in the ALFALFA Dwarf sample as a function of local density. We find that void galaxies are on average more isolated than wall galaxies. Redshift space distributions show that H I selected galaxies in ALFALFA rarely appear in clusters, as seen in figure 5 of Moorman et al. (2014).

than in voids. Because SSFR and color are strongly correlated, these authors make the claim that SSFRs must be lower in denser regions.

At first glance, the recent results of Ricciardelli et al. (2014) appear to contradict our results, although this is likely a consquence of how the authors define "void" in their work. Ricciardelli et al. (2014) estimate the SSFR of "void" and "shell" galaxies within the SDSS DR7. These authors find that the average SSFR does *not* vary with large-scale structure. These results do not necessarily contradict our results, because the definitions of LSS used in that work vary from what we define in this work. The "void" galaxy sample used in Ricciardelli et al. (2014) is a sample of galaxies that live only in the void centers. That is, the authors use a void catalog that only includes the "maximal sphere" of each void. Assuming voids are non-spherical bodies comprised of multiple spheres to create an ellipsoidal shape, the "maximal sphere" of a void, is simply the sphere with the maximum radius within a single void. This allows the authors to use only galaxies in the void centers; however, they are comparing their void sample to a "shell" sample that likely contains void galaxies from the outskirts of the voids. Pan et al. (2012) show that the density profiles of voids are flat out to the edges, therefore properties of galaxies should not vary with void centric

distance. The "shells" used in this paper are spherical shells from the maximal sphere radius, $R_{void}$, to $1.5R_{void}$. If all voids were perfectly spherical, this would work well to distinguish galaxies in underdense versus dense regions, but Pan (2011) shows that voids in the nearby Universe are more ellipsoidal than spherical, with a tendency towards bring prolate. By accounting for only the maximal spheres of a void, these authors are using a sample littered with both void and wall galaxies as the "shell" sample. Comparing properties of void galaxies with a population that likely has a significant number of void galaxies mixed in, they would not notice a difference. It is clear from their distributions that they are lacking a large portion of quiescent galaxies that are present in our sample. Consistent with our findings, these authors find that the proportion of star forming galaxies in voids is higher and the fraction of passive galaxies are higher in denser regions.

The SSFR trends seen in our work also agree with the high-resolution void simulation of Cen (2011), who predicts that void galaxies will have higher SSFRs than galaxies in denser regions. Cen (2011) also finds a trend of increasing SSFRs with decreasing stellar mass. As we move into the dwarf regime, we find that galaxies with lower $M_*$ have higher SSFRs, with most (90% void dwarf galaxies and 85% of wall dwarf galaxies) having SSFRs high enough to double the stellar mass within a Hubble time, according to the $FUV$ method.

Our results on the SSFRs of ALFALFA galaxies are also in agreement with the results of Kreckel et al. (2012) regarding the environmental dependence of SSFR in an H I selected sample. Kreckel et al. (2012) use the Void Galaxy Survey (VGS), a targeted H I imaging survey, to map the H I in galaxies in known voids in the nearby Universe. They compare 60 void galaxies from the VGS to a control sample of galaxies in average environments in a similar stellar mass range from the GALEX Arecibo SDSS Survey (GASS) catalog. They find that the SSFRs of H I selected void galaxies are similar to SSFRs of galaxies in denser regions. While we find higher SSFRs in void galaxies for our NSA sample, the void and stellar mass-matched wall SSFRs of ALFALFA galaxies are very similar. Beygu et al. (2015) also use the VGS and find no difference in SSFR between VGS void galaxies and galaxies of similar stellar mass in denser environments (JCMT field galaxies, LV isolated and field galaxies, and ALFALFA Virgo cluster galaxies). The Galex Arecibo SDSS Survey (GASS) Data Release 3 (Catinella et al. 2013) compares the SSFRs of a 760 galaxy sample across environments and finds that star formation is quenched at the group environments. The H I sensitivity of this survey is higher than that of ALFALFA, however the GASS survey is designed to be complete at stellar masses above $10^{10}M_{\odot}$, a regime which includes only the highest decade of objects that we analyze.

Most works to date investigating the environmental dependence of star formation efficiencies have focused on clusters or isolated galaxies rather than on large-scale void environments. One work that does focus on the LSS dependence of SFEs is that of Kreckel et al. (2012), who find only two galaxies within the VGS with $M_* > 10^{10}M_{\odot}$ which they could compare to the GASS galaxies in denser regions. These two galaxies have higher SFEs ($10^{-8.6}\mathrm{yr}^{-1}$ and $10^{-9.1}\mathrm{yr}^{-1}$) than $M_* > 10^{10}M_{\odot}$ GASS galaxies which had an average SFE of $10^{-9.5}\mathrm{yr}^{-1}$ in this stellar mass range. Kreckel et al. (2012) further compare the VGS SFEs to a volume-limited sample of 447 ALFLFA

galaxies ($\log(M_{HI}) > 9$ within $0.007 < z < 0.024$). The 447 ALFALFA control galaxies live in average density regions ($1 < \delta + 1 < 10$) and are crossmatched to SDSS DR7 using cross-matching techniques found in Toribio et al. (2011). The authors find hints (via a weak trend) that the VGS galaxies display higher SFEs than the volume-limited ALFALFA subset, but do not suggest that these results are significant. Our results for the full ALFALFA sample do not indicate that void galaxies, on the whole, are more effective at forming stars with their gas. This is in agreement with the analysis of Kreckel et al. (2011) who analyze the void simulation of Cen (2011) and find that SFEs in voids are similar to those in denser regions across all magnitudes except in the dwarf galaxy regime. Further investigation of the VGS void galaxies by Beygu et al. (2015) reveals no difference in SFE between VGS void galaxies and galaxies of similar stellar mass in denser regions (JCMT field galaxies, LV isolated and field galaxies, and ALFALFA Virgo cluster galaxies).

Investigating the ALFALFA Dwarf SFE distributions, we find that the low-SFE end appears to have relatively more void galaxies than wall galaxies. This could be indicative of lower SFEs in voids, but is not statistically significant. If it is the case that void galaxies have lower SFEs, this would be in agreement with the work of Bigiel et al. (2010) who find that the H I column is correlated with SFE and is dependent on local environment. It may be the case that even small-scale groups of galaxies within voids provide a more isolated environment (i.e. lower $\delta$) than even the most isolated of galaxies outside of voids. See Figure 10 which shows that void dwarf galaxies are significantly more isolated than wall dwarf galaxies.

## 8. CONCLUSIONS

We examine the effects of both large-scale and local environment on star formation properties of these two samples, focusing particularly on the faintest galaxies ($M_r \geq -17$). We utilize the NASA Sloan Atlas (NSA) which offers a set of cross-matched objects within the SDSS DR8-GALEX-ALFALFA footprint. From the NSA sample, we extract 113,145 galaxies with optical and UV information, and 8070 galaxies with information from all three catalogs. We determine the large-scale environment in which each galaxy lives using the void catalog of Pan et al. (2012) splitting the galaxies into "void galaxies" and "wall galaxies." We match the stellar mass distributions of void and wall galaxies (thus controlling for the strong shift toward smaller galaxy mass in voids) and find the following results.

- Void dwarf ($M_r \geq -17$) galaxies have higher SSFRs than wall dwarf galaxies. The trend towards higher SSFRs in voids holds true on star formation timescales of both $\sim$ 10 and $\sim$ 100 Myr, using SFR estimates from H$\alpha$ lines and $FUV$ photometry, respectively. We reproduce the trend towards higher SSFRs for bright void galaxies and reveal that the shift towards higher SSFRs in cosmic voids extends down to magnitudes as faint as $M_r = -13$.
- When we limit our sample to galaxies containing enough H I to be detected by ALFALFA, we remove the passive galaxy population. After stellar mass matching the void and wall

ALFALFA galaxies, we notice no difference in the SSFR distributions. This further supports the finding that ALFALFA detects primarily blue, star forming galaxies.

- Comparing only the active star forming sequences in the NSA and ALFALFA catalogs shows a shift towards lower SSFRs in ALFALFA. It is possible that H I selected galaxies are more dust-reddened on average than optically selected star forming galaxies. This result is consistent with the finding in Moorman et al. (2015) that the blue cloud in ALFALFA is somewhat redder than the blue cloud of the optically selected sample. Figure 1 in Moorman et al. (2015) shows a similar shift of the blue cloud towards redder colors than the blue cloud galaxy distribution of the optically selected sample.

- Investigating the dwarf galaxy population within the NSA and ALFALFA samples, we find that dwarf galaxies have higher SSFRs and lower SFEs than typical brighter galaxies. This indicates that dwarf galaxies are likely to be actively forming stars at a relatively high rate. The lower SFEs could also imply that dwarf galaxies are able to retain their gas more easily than brighter galaxies (lower SFEs are caused by large H I masses rather than low SFRs in the ratio SFE=SFR/$M_{HI}$).

- We do not find statistical evidence that the void environment has an impact on the SFEs of dwarf galaxies. This is unsurprising, given that galaxies in our void and wall samples have strong H I emission and similar stellar mass distributions. Assuming that the two samples *are* drawn from the same distribution, it would appear that the wall dwarf sample is lacking galaxies around log(SFE)$\sim -10$. Dwarf galaxies have been forming stars at relatively high rates in recent times (10Myr), but due to survey sensitivities, we can only see dwarf galaxies in the very nearby Universe. Because it is difficult to identify true voids in the nearby volume, we are unable to make a statistically significant comparison of the star formation efficiencies of void dwarf and wall dwarf galaxies.

## Acknowledgments

The authors would like to acknowledge the work of the entire ALFALFA collaboration team in observing, flagging, and extracting the catalog of galaxies used in this work. The ALFALFA team at Cornell is supported by NSF grants AST-0607007 and AST-1107390 to RG and MPH and by grants from the Brinson Foundation. This study was supported by NSF grant AST-1410525 at Drexel University. We thank the referee for their helpful comments.

The NASA-Sloan Atlas was created by Michael Blanton, with extensive help and testing from Eyal Kazin, Guangtun Zhu, Adrian Price-Whelan, John Moustakas, Demitri Muna, Renbin Yan and Benjamin Weaver. Renbin Yan provided the detailed spectroscopic measurements for each SDSS spectrum. David Schiminovich kindly provided the input GALEX images. We thank Nikhil Padmanabhan, David Hogg, Doug Finkbeiner and David Schlegel for their work on SDSS image infrastructure.

We acknowledge the support of NASA, the Centre National d'Etudes Spatiales (CNES) of France, and the Korean Ministry of Science and Technology for the construction, operation, and data analysis of the GALEX mission.

Funding for the creation and distribution of the SDSS Archive has been provided by the Alfred P. Sloan Foundation, the Participating Institutions, the National Aeronautics and Space Administration, the National Science Foundation, the U.S. Department of Energy, the Japanese Monbukagakusho, and the Max Planck Society. The SDSS Web site is http://www.sdss.org/.

The SDSS is managed by the Astrophysical Research Consortium (ARC) for the Participating Institutions. The Participating Institutions are The University of Chicago, Fermilab, the Institute for Advanced Study, the Japan Participation Group, The Johns Hopkins University, the Korean Scientist Group, Los Alamos National Laboratory, the Max-Planck-Institute for Astronomy (MPIA), the Max-Planck-Institute for Astrophysics (MPA), New Mexico State University, University of Pittsburgh, Princeton University, the United States Naval Observatory, and the University of Washington.

## REFERENCES

Aihara, H., Allende Prieto, C., An, D., et al. 2011, ApJS, 195, 26

Alpaslan, M., Driver, S., Robotham, A. S. G., et al. 2015, ArXiv e-prints, arXiv:1505.05518

Benson, A. J., Lacey, C., Baugh, C., Cole, S., & Frenk, C. 2002, in Astronomical Society of the Pacific Conference Series, Vol. 254, Extragalactic Gas at Low Redshift, ed. J. S. Mulchaey & J. T. Stocke, 354

Beygu, B., Kreckel, K., van der Hulst, J. M., et al. 2015, ArXiv e-prints, arXiv:1501.02577

Bigiel, F., Leroy, A., Walter, F., et al. 2010, AJ, 140, 1194

Blanton, M. R., Kazin, E., Muna, D., Weaver, B. A., & Price-Whelan, A. 2011, AJ, 142, 31

Blanton, M. R., Lin, H., Lupton, R. H., et al. 2003, AJ, 125, 2276

Blanton, M. R., & Roweis, S. 2007, AJ, 133, 734

Bruzual, G., & Charlot, S. 2003, MNRAS, 344, 1000

Catinella, B., Schiminovich, D., Kauffmann, G., et al. 2010, MNRAS, 403, 683

Catinella, B., Schiminovich, D., Cortese, L., et al. 2013, MNRAS, 436, 34

Cen, R. 2011, ApJ, 741, 99

Choi, Y.-Y., Han, D.-H., & Kim, S. S. 2010, Journal of Korean Astronomical Society, 43, 191

da Costa, L. N., Pellegrini, P. S., Sargent, W. L. W., et al. 1988, ApJ, 327, 544

El-Ad, H., & Piran, T. 1997, ApJ, 491, 421

Elbaz, D., Daddi, E., Le Borgne, D., et al. 2007, A&A, 468, 33

Fukugita, M., Ichikawa, T., Gunn, J. E., et al. 1996, AJ, 111, 1748

Geller, M. J., & Huchra, J. P. 1989, Science, 246, 897

Giovanelli, R., Haynes, M. P., Kent, B. R., et al. 2005a, AJ, 130, 2598

—. 2005b, AJ, 130, 2613

Goldberg, D. M., Jones, T. D., Hoyle, F., et al. 2005, ApJ, 621, 643

Goldberg, D. M., & Vogeley, M. S. 2004, ApJ, 605, 1

Gunn, J. E., Carr, M., Rockosi, C., et al. 1998, AJ, 116, 3040

Haynes, M. P., Giovanelli, R., Martin, A. M., et al. 2011, AJ, 142, 170

Hoeft, M., Yepes, G., Gottlöber, S., & Springel, V. 2006, MNRAS, 371, 401

Hopkins, A. M., Miller, C. J., Nichol, R. C., et al. 2003, ApJ, 599, 971

Hoyle, F., Rojas, R. R., Vogeley, M. S., & Brinkmann, J. 2005, ApJ, 620, 618

Hoyle, F., & Vogeley, M. S. 2002, ApJ, 566, 641

Hoyle, F., Vogeley, M. S., & Pan, D. 2012, MNRAS, 426, 3041

Huang, S., Haynes, M. P., Giovanelli, R., & Brinchmann, J. 2012a, ApJ, 756, 113

Huang, S., Haynes, M. P., Giovanelli, R., et al. 2012b, AJ, 143, 133

Icke, V. 1984, MNRAS, 206, 1P

Karachentsev, I. D., Karachentseva, V. E., Huchtmeier, W. K., & Makarov, D. I. 2004, AJ, 127, 2031

Kennicutt, Jr., R. C. 1998, ARA&A, 36, 189

Koposov, S. E., Yoo, J., Rix, H.-W., et al. 2009, ApJ, 696, 2179

Kreckel, K., Joung, M. R., & Cen, R. 2011, ApJ, 735, 132

Kreckel, K., Platen, E., Aragón-Calvo, M. A., et al. 2012, AJ, 144, 16

Lee, J. C., Gil de Paz, A., Tremonti, C., et al. 2009, ApJ, 706, 599

Lupton, R., Gunn, J. E., Ivezić, Z., Knapp, G. R., & Kent, S. 2001, in Astronomical Society of the Pacific Conference Series, Vol. 238, Astronomical Data Analysis Software and Systems X, ed. F. R. Harnden, Jr., F. A. Primini, & H. E. Payne, 269

Martin, D. C., Fanson, J., Schiminovich, D., et al. 2005, ApJ, 619, L1

Moorman, C. M., Vogeley, M. S., Hoyle, F., et al. 2014, MNRAS, 444, 3559

—. 2015, ApJ, 810, 108

Pan, D. C. 2011, PhD thesis, Drexel University

Pan, D. C., Vogeley, M. S., Hoyle, F., Choi, Y.-Y., & Park, C. 2012, MNRAS, 421, 926

Ricciardelli, E., Cava, A., Varela, J., & Quilis, V. 2014, MNRAS, 445, 4045

Rojas, R. R., Vogeley, M. S., Hoyle, F., & Brinkmann, J. 2005, ApJ, 624, 571

Salim, S., Rich, R. M., Charlot, S., et al. 2007, ApJS, 173, 267

Stanonik, K., Platen, E., Aragón-Calvo, M. A., et al. 2009, ApJ, 696, L6

Strauss, M. A., Weinberg, D. H., Lupton, R. H., et al. 2002, AJ, 124, 1810

Toribio, M. C., Solanes, J. M., Giovanelli, R., Haynes, M. P., & Masters, K. L. 2011, ApJ, 732, 92

van de Weygaert, R., & van Kampen, E. 1993, MNRAS, 263, 481

von Benda-Beckmann, A. M., & Müller, V. 2008, MNRAS, 384, 1189

Willick, J. A., Courteau, S., Faber, S. M., et al. 1997, ApJS, 109, 333

Yan, R. 2011, AJ, 142, 153

Yan, R., & Blanton, M. R. 2012, ApJ, 747, 61

York, D. G., Adelman, J., Anderson, Jr., J. E., et al. 2000, AJ, 120, 1579

This preprint was prepared with the AAS LaTeX macros v5.2.

Table 2. Gaussian fits to the SFEs

| Sample | type | method | $A_1$ | $\mu_1$ | $\sigma_1$ | $A_2$ | $\mu_2$ | $\sigma_2$ |
|---|---|---|---|---|---|---|---|---|
| ALFALFA | void | H$\alpha$ | 500 | -10.530 | 0.646 | -3 | -11.558 | 1.138 |
| ALFALFA | wall | H$\alpha$ | 499 | -10.492 | 0.607 | 7 | -7.618 | 1.894 |
| ALFALFA Dwarf | void | H$\alpha$ | 72 | -10.611 | 0.701 | -2 | -5.956 | 0.521 |
| ALFALFA Dwarf | wall | H$\alpha$ | 66 | -10.776 | 0.493 | 13 | -9.488 | 0.374 |
| ALFALFA | void | *FUV* | 874 | -9.986 | 0.361 | — | — | — |
| ALFALFA | wall | *FUV* | 805 | -9.989 | 0.3759 | — | — | — |
| ALFALFA Dwarf | void | *FUV* | 125 | -10.038 | 0.339 | 28 | -10.658 | 0.284 |
| ALFALFA Dwarf | wall | *FUV* | 43 | -10.281 | 0.240 | 56 | -10.082 | 0.498 |